Janik Schaude*, Julius Albrecht, Ute Klöpzig, Andreas C. Gröschl and Tino Hausotte

Atomic force microscope with an adjustable probe direction and piezoresistive cantilevers operated in tapping-mode

Im Tapping-Modus betriebenes Rasterkraftmikroskop mit einstellbarer Antastrichtung und piezoresistiven Cantilevern

DOI 10.1515/teme-2019-0035

Abstract: This article presents a new tilting atomic force microscope (AFM) with an adjustable probe direction and piezoresistive cantilever operated in tapping-mode. The AFM is based on two rotational axes, which enable the adjustment of the probe direction to cover a complete hemisphere. The whole setup is integrated into a nano measuring machine (NMM-1) and the metrological traceability of the piezoresistive cantilever is warranted by in situ calibration on the NMM-1. To demonstrate the capabilities of the tilting AFM, measurements were conducted on a step height standard.

Keywords: Atomic force microscopy, tilting AFM, piezoresistive cantilever, nano measuring machine.

Zusammenfassung: In diesem Artikel wird ein neues, drehbares Rasterkraftmikroskop mit einstellbarer Antastrichtung und piezoresistivem Cantilever vorgestellt, welches im Tapping-Modus betrieben wird. Das Rasterkraftmikroskop ist auf zwei rotatorischen Achsen platziert, wodurch eine Anpassung der Antastrichtung auf einer kompletten Hemisphäre ermöglicht wird. Der gesamte Aufbau ist in die Nanomessmaschine NMM-1 integriert und die metrologische Rückführbarkeit des piezoresistiven Cantilevers wird durch in situ Kalibrierungen auf der NMM-1 sichergestellt. Um die Fähigkeiten des drehbaren Rasterkraftmikroskops zu demonstrieren, wurden Messungen an einem Stufenhöhennormal durchgeführt.

Keywords: Rasterkraftmikroskopie, piezoresistive Cantilever, Nanomessmaschine.

***Corresponding author: Janik Schaude,** Institute of Manufacturing Metrology, Friedrich-Alexander-University Erlangen-Nuremberg (FAU), Nägelsbachstr. 25, 91054 Erlangen, E-Mail: janik.schaude@fmt.fau.de

Julius Albrecht, Ute Klöpzig, Andreas C. Gröschl, Tino Hausotte, Institute of Manufacturing Metrology, Friedrich-Alexander-University Erlangen-Nuremberg (FAU), Nägelsbachstr. 25, 91054 Erlangen

1 Introduction and literature review

Since its invention in 1986 [2] the AFM has become a widely used and traceable tool in nanometrology. The still ongoing development led to different approaches to measure the deflection of the cantilever [22]. While the optical beam deflection (OBD) method is still mainly used, the once inferior signal-to-noise ratio (SNR) of self-sensing methods, like the piezoresistive deflection measurement [21], has been improved steadily and is nowadays comparable to the SNR of OBD [6].

Besides the deflection detection, the measurement of vertical or near vertical surface features, features with a high-aspect-ratio or even undercut features is another important field of research. One approach is to use boot-shaped cantilever-tips [13] for critical dimension (CD)-AFM. While sidewalls are well resolved by this method, the shape of the tip leads to a poor resolution of the flat parts of the feature. Furthermore, tip characterization and the subsequent correction of the dilation caused by the finite tip size is quite laboriously, since measurements are conducted at the whole circumference of the tip [4]. Another approach is to introduce an inclination between the measuring object and the cantilever. This might be done by tilting the sample [7, 8], or by tilting the cantilever in one direction [3, 11].

The new AFM presented here is based on two rotational axes [17], which enable the adjustment of the probe direction to cover a complete hemisphere. The sensor utilizes self-sensing piezoresistive cantilevers [19] and is operated in tapping-mode. Therefore, a piezoelectric drive [16] stimulates the cantilever near its resonance frequency. The whole setup is installed in a NMM-1 with a motion range of 25 mm x 25 mm x 5 mm and a resolution of 0.1 nm [9].

2 Setup

2.1 Hardware setup

The setup of the sensor is shown schematically in fig. 1 and integrated into the NMM-1 in fig. 2. The first axis (1 and 2), an Aerotech ANT95R-180 with a positioning range of 180° [1], is oriented parallel to the z-axis of the NMM-1. The second axis (3 and 4), a SmarAct SR-2812 with a positioning range of 360° [20], is mounted under an angle of 45°. A flexure hinge (6) connects the second axis with the socket for the self-sensing cantilever (7). The piezoelectric drive (5) stimulates the cantilever to operate the AFM in tapping-mode. The power supply of the Wheatstone bridge on the cantilever and the measuring signal are transduced by a flexible printed circuit board (PCB). The cantilever tip is located as close as possible to the intersection point of both rotary axes, minimizing the translational movement of the tip when rotating the axes.

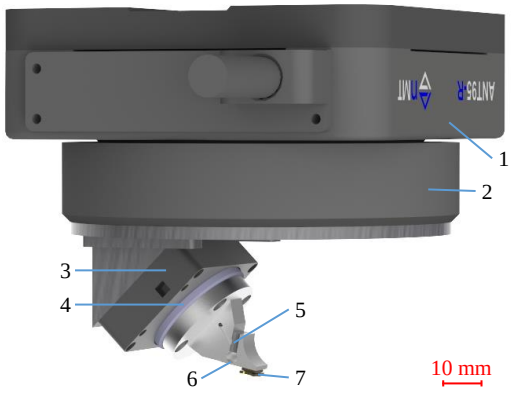

Fig. 1: Schema of the setup: 1 static part of the first axis; 2 moveing part of the first axis; 3 static part of the second axis; 4 moveing part of the second axis; 5 piezoelectric drive; 6 flexure hinge; 7 self-sensing cantilever.

2.2 Signal processing

The signal evaluation is conducted with a Zurich Instruments HF2LI lock-in amplifier [23]. The reference signal is impedance converted by a current feedback amplifier [12] and stimulates the piezoelectric drive near the cantilever's resonance frequency. The signal of the piezoresistive self-sensing cantilever is amplified by a commercial pre-amplifier [18] and transduced to the lock-in amplifier,

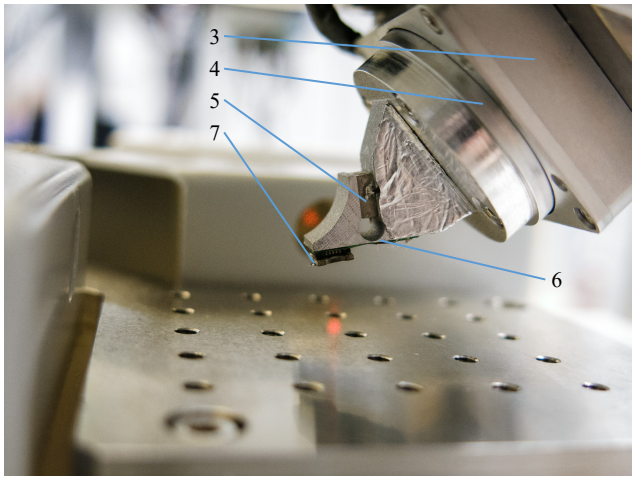

Fig. 2: Setup integrated into the NMM-1: 3 static part of the second axis; 4 moveing part of the second axis; 5 piezoelectric drive; 6 flexure hinge; 7 self-sensing cantilever.

which calculates the phase-independent amplitude of the oscillation. This amplitude is the measuring signal and feedback signal passed to the NMM-1 to control the x-, y- and z-axis according to the probe direction specified in the measuring command.

3 Calibration

To ensure the metrological traceability of the piezoresistive cantilever, it is calibrated on the NMM-1. Firstly, the second axis is in its zero position and the probe direction is the direction of the z-axis of the NMM-1. Therefore, the calibration is done against the traceable z-interferometer. The cantilever used is stimulated with a frequency of 322.1 kHz and therefore slightly higher than its free resonance frequency. The calibration is conducted 40 times within a period of time of 70 s in order to determine the short-term precision of the sensor. For each calibration the characteristic curve $d_{\mathrm{AFM}}(V)$, where d_{AFM} is the deflection of the cantilever and V is the measuring signal, is fitted as cubic polynomial. The mean range of the characteristic curves is 89 nm. In fig. 3 the deviation $\Delta z = d_{\mathrm{AFM}}(V) - z_{\mathrm{NMM}}$ is shown, where $d_{\mathrm{AFM}}(V)$ is calculated by the first characteristic curve. Depicted in red are the residues of the characteristic curve, for which there is no systematic deviation perceptible. The deviations to the other 39 calibrations are shown in green. To determine the measurement repeatability of the sensor, every characteristic curve is applied to the measuring points of every calibration and Δz is calculated. The standard deviation of Δz is 1.8 nm.

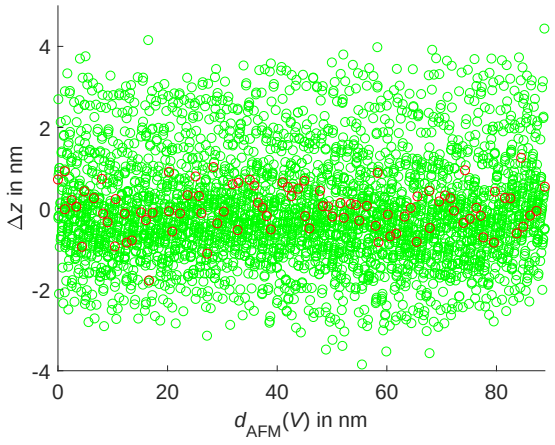

Fig. 3: Deviations of the deflection of the cantilever to the z-values of the NMM-1 for 40 calibrations. Residues of the characteristic curve are shown in red.

4 Measurement of a calibration grating

Measurements are conducted on a calibration grating with a step height of (21.4 ± 1.5) nm and a period P of (3.0 ± 0.01) µm [15]. The grating is put on the NMM-1 under an angle of about $-\frac{\pi}{4}$ (-45°) compared to the xz-plane of the reference coordinate system of the NMM-1 and therefore in direction of the cantilever. Methods to determine the workpiece coordinate system (WCS) of a calibration grating have been reported in [5, 14]. In this paper the profile height (z_{WCS}) is calculated by calculating $-z_{\mathrm{NMM}} + d_{\mathrm{AFM}}$ and tilting this difference by calculating for each measurement point the perpendicular distance to the linear regression of all measurement points $-z_{\mathrm{NMM}} + d_{\mathrm{AFM}}$.

4.1 Determination of the workpiece coordinate system

The period of the calibration grating must be measured perpendicular to the grating lines. Therefore an accurate determination of the WCS is mandatory. To determine the WCS, two scans are conducted on the grating with a point distance of 0.5 nm, a velocity of 2 µm/s and a scan length of 500 µm. One scan is conducted under an angle of $-\frac{\pi}{4} + \frac{\pi}{12}$ (-30°) and the other under an angle of $-\frac{\pi}{4} + \frac{\pi}{6}$ (-15°). For both scans the periods P_1 and P_2 are calculated with Fourier analysis (cf. fig. 4). The unknown angle β between the first scan and the line perpendicular to the gratings is calculated with P_1, P_2 and φ, which is the angle between the first and the second scan, ca. $\frac{\pi}{12}$ (15°) in this case. As shown in fig. 4, $\cos(\beta) = \frac{P}{P_2}$ and $\cos(\beta + \varphi) = \frac{P}{P_1}$, which leads to $\frac{P_2}{P_1} = \frac{\cos(\beta+\varphi)}{\cos(\beta)}$. By substituting $\cos(\beta + \varphi)$ with $\cos(\beta)\cos(\varphi) - \sin(\beta)\sin(\varphi)$ and $\frac{\sin(\beta)}{\cos(\beta)}$ with $\tan(\beta)$, the formula becomes $\frac{P_2}{P_1} = \cos(\varphi) - \tan(\beta)\sin(\varphi)$, which leads to $\beta = \arctan(\frac{\cos(\varphi) - \frac{P_2}{P_1}}{\sin(\varphi)})$.

For the measurements conducted, φ is 0.84° larger than β, therefore the angle between the grating and the xz-plane of the NMM-1's coordinate system is 44.16°. Measuring along the line perpendicular to the grating lines, Fourier analysis results in a measured period P_{M} of 2.994 µm, which agrees well with the nominal value.

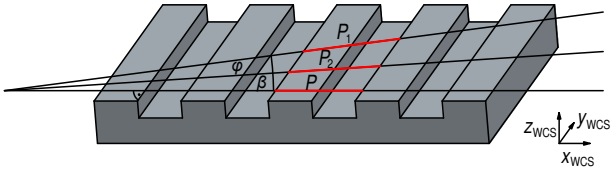

Fig. 4: Determination of the workpiece coordinate system.

4.2 Scan velocity

Because of the low-pass filtering associated with the calculation of the phase-independent amplitude of the oscillation, a latency between the signals of the intererometers of the NMM-1 and the measuring signal is inevitable. The effects increase with an increasing scan velocity and are quantified by measuring a single step forwards and backwards with different velocities and by comparing the measuring results. This is possible since z_{WCS} takes into account d_{AFM} and z_{NMM}. As shown in fig. 5, for a velocity of 30 µm/s the lateral mismatch between forwards and backwards scan Δx_{WCS} is about 70 nm, while for a velocity of 5 µm/s the mismatch is below the dispersion.

4.3 Determination of the step height

To determine the step height, one measurement is conducted perpendicular to the gratings with a point distance of 0.5 nm, a velocity of 5 µm/s and a scan length of 100 µm. The in accordance with ISO 5436 [10] calculated

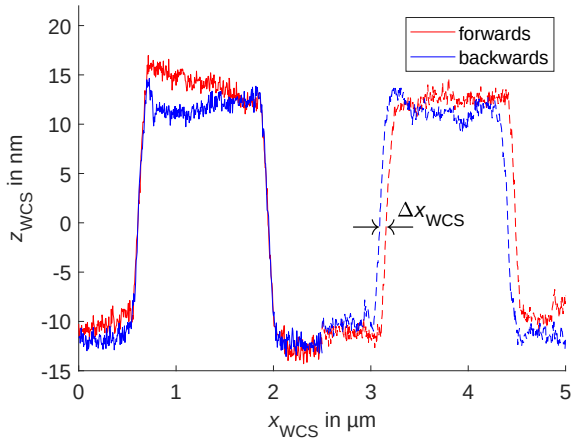

Fig. 5: One single step measured forwards and backwards with a velocity of 5 µm/s (solid line) and 30 µm/s (dashed line).

step height is 24.2 nm and therefore 2.8 nm higher than the nominal value. This deviation was caused by a lateral mismatch of the probing point and the Abbe-point (intersection point of the axes of the three interferometers) of the NMM-1. Since a collision of the sensor and the corner-mirror must be avoided, it is not possible to align the probing point and the Abbe-point. Nevertheless, placing the sensor over the corner-mirror and therefore aligning the probing point and the Abbe-point laterally and misaligning it in the z-direction of the NMM-1 proved to be more advantageous, since a repeated measurement with this configuration led to a step height of 20.7 nm. While the measurements of section 5.2 have been conducted in this preverable configuration, the measurements of section 5.1 have been completed with the lateral misalignment.

5 Adjustment of the probe direction

5.1 Rotation of the first axis

After the rotation of the first axis by 180°, the sensor is again calibrated and the standard deviation is determined similar to the approach presented in section 3. The obtained standard deviation is 1.4 nm. The WCS of the grating is determined similar to the approach of section 4.1. The angle between the grating and the NMM-1 is 44.35° and the measured period is 2.994 µm. The measured step height is 24.1 nm. All the values obtained agree well with the values before the rotation. The good agreement between both measurements is also shown in fig. 6, where three steps are depicted. To compensate for the translational movement associated with the rotation of the first axis, both measurements are aligned at their edges.

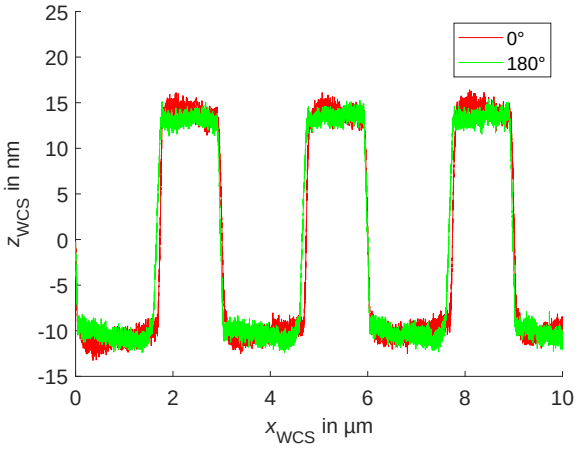

Fig. 6: Measurement of the calibration grating for two positions of the first rotary axis.

5.2 Rotation of the second axis

By rotating the second axis it is possible to adjust the angle between the probe direction and the xy-plane of the NMM-1, which is favourable if the surface normal of the measuring object is not parallel to the z-axis of the NMM-1. To demonstrate this, the calibration grating is placed on the NMM-1 under an angle of about 27° and the second axis is rotated accordingly. Contrary to the previous measurements, in this case the measuring direction has to be perpendicular to the cantilever, while it was in line with the cantilever, previously. To evaluate the impact of this, one measurement with the grating placed in the xy-plane of the NMM-1 and the second axis set to its zero position, but with the measuring direction perpendicular to the cantilever, is prepended. Three steps of the grating measured when placed in the xy-plane of the NMM-1 and placed with an angle of 27° and the second axis rotated accordingly are shown in fig. 7. Measuring the tilted grating without tilting the cantilever was not possible, since the mounting of the cantilever touches the grating prior to the cantilever itself. The step height is 20.4 nm for the flat grating and 20.7 nm for the tilted grating, which agrees well with the nominal value and the value obtained in section 4.3 with the probing point and the Abbe-point aligned laterally.

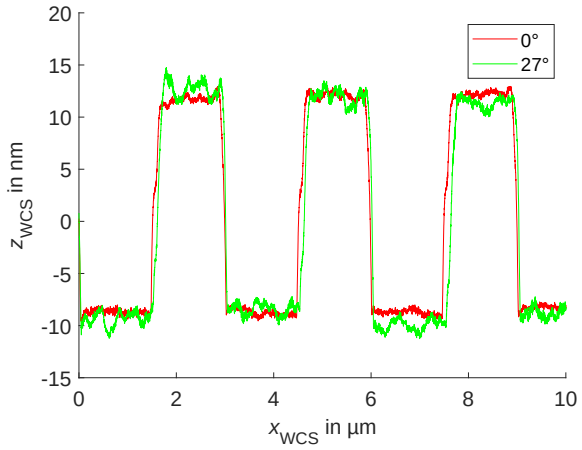

Fig. 7: Measurement of the calibration grating placed in the xy-plane of the NMM-1 and tilted by 27°.

6 Summary and outlook

In this article a new tilting AFM has been presented. The sensor has demonstrated a high measurement repeatability for the calibrations on the NMM-1. Furthermore, with the second axis it is possible to measure objects with a surface normal that is not parallel to the z-axis of the NMM-1. The measuring results of the tilted calibration grating are in very good agreement with the results obtained for the not-tilted calibration grating, if the probe direction is aligned to the surface normal of the grating. So far, the measurement points taken with different probe directions were stitched using algorithms that rely on characteristic features of the measuring object. In future works the translational movement of the sensor associated with the rotation of the axes shall be determined in order to merge these measurement points.

Acknowledgment: This project has received funding from the EMPIR programme co-financed by the Participating States and from the European Union's Horizon 2020 research and innovation programme. The authors wish to thank for the funding.

References

[1] *ANT95R, Single-Axis Rotary Direct-Drive Nanopositioning Stages, Manual*. Aerotech, without a year.

[2] G. Binnig and C. Quate. Atomic Force Microscope. *Physical Review Letters*, 56(9):930–934, 1986.

[3] S.-J. Cho, B.-W. Ahn, J. Kim, J.-M. Lee, Y. Hua, Y. K. Yoo, and S. Park. Three-dimensional imaging of undercut and sidewall structures by atomic force microscopy. *Review of Scientific Instruments*, 82(23707), 2011.

[4] G. Dahlen, M. Osborn, H. Liu, R. Jain, W. Foreman, and J. R. Osborne. Critical Dimension AFM tip characterization and image reconstruction applied to the 45 nm node. *Proc. SPIE 6152, Metrology, Inspection, and Process Control for Microlithography XX*, 2006.

[5] G. Dai, F. Pohlenz, T. Dziomba, M. Xu, A. Diener, L. Koenders, and H.-U. Danzebring. Accurate and traceable calibration of two-dimensional gratings. *Meas. Sci. Technol.*, 18(2), 2007.

[6] M. Dukic, J. D. Adams, and G. E. Fantner. Piezoresistive AFM cantilevers surpassing standard optical beam deflection in low noise topography imaging. *Scientific Reports*, 5 (16393), 2015.

[7] M. Fouchier, E. Pargon, and B. Bardet. An atomic force microscopy-based method for line edge roughness measurement. *Journal of Applied Physics*, 113(104903), 2013.

[8] J. Garnaes, P.-E. Hansen, N. Agersnap, I. Davi, J. C. Petersen, A. Kuehle, J. Holm, and L. H. Christensen. Determination of sub-micrometer high aspect ratio grating profiles. *Proc. SPIE 5878, Advanced Characterization Techniques for Optics, Semiconductors, and Nanotechnologies II*, 2005.

[9] T. Hausotte, B. Percle, and G. Jäger. Advanced three-dimensional scan methods in the nanopositioning and nanomeasuring machine. *Meas. Sci. Technol.*, 20(8):1–8, 2009.

[10] ISO 5436-1:2000. *Geometrical product specifications (GPS) – Surface texture: Profile method; Measurement standards - Part 1: Material measures*.

[11] R. Kizu, I. Misumi, A. Hirai, K. Kinoshita, and S. Gonda. Development of a metrological atomic force microscope with a tip-tilting mechanism for 3D nanometrology. 29(7), 2018.

[12] *LT1206, Manual*. Linear Technology, 1993.

[13] Y. Martin and H. K. Wickramasinghe. Method for imaging sidewalls by atomic force microscopy. *Appl. Phys. Lett.*, 64: 2498–2500, 1994.

[14] I. Misumi, S. Gonda, T. Kurosawa, and K. Takamasu. Uncertainty in pitch measurements of one-dimensional grating standards using a nanometrological atomic force microscope. *Meas. Sci. Technol.*, 14(4), 2003.

[15] *Calibration grating TGZ1, Manual*. NT - MDT Co., Building 167, Zelenograd, Moscow 124460, Russia, 2018.

[16] *PICMA® Chip Aktoren, Manual*. PI, 2017.

[17] A. Schuler, A. Weckenmann, and T. Hausotte. Enhanced measurement of high aspect ratio surfaces by applied sensor tilting. *Acta IMEKO*, 3(3), 2014.

[18] *Pre-Amplifier Kit, Manual*. SCL-Sensor.Tech. Fabrication GmbH, 2017.

[19] *Silicon piezo-resistive sensing cantilevers, Manual*. SCL-Sensor.Tech. Fabrication GmbH, 2018.

[20] *Product Catalog*. SmarAct, 2016.

[21] M. Tortonese, H. Yamada, R. C. Barrett, and C. F. Quate. Atomic force microscopy using a piezoresistive cantilever. *Transducers '91: Int. Conf. on Solid-State Sensors and Actuators*, pages 448–451, 1991.

[22] A. Yacoot and L. Koenders. Recent developments in dimensional nanometrology using AFMs. *Meas. Sci. Technol.*, 22 (12), 2011.

[23] *HF2LI 50 MHz Lock-in Amplifier, Manual*. Zurich Instruments, 2019.